NATIONAL ACADEMY OF SCIENCES OF BELARUS

INSTITUTE OF MATHEMATICS

Second International Conference

"FINITE-DIFFERENCE METHODS: THEORY AND APPLICATION"

(CFDM98)

PROCEEDINGS

Volume 2

EDITED BY
A.A.SAMARSKII

Minsk, Belarus

SOLUTION OF TWO-DIMENSIONAL STEFAN PROBLEM BY THE METHOD OF DYNAMIC ADAPTATION [1]

V.I.MAZHUKIN

Institute of Mathematical Modeling, RAS, 4 Miusskaya Square, 125047 Moscow, Russia
phone (095) 974-59-41, fax (095) 974-59- 41,
e-mail: mazhukin@imm.msk.ru

M.M.CHUIKO

Institute of Mathematics, NASB, 11 Surganov St., 220072 Minsk, Belarus
phone (017) 284-19-53, fax (017) 284-09- 15,
e-mail: dns@im.bas-net.by

Application of the dynamic adaptation method for the solution of two-dimensional Stefan problem with explicit tracking of the interface is considered. The comparison of numerical and analytical solutions for the freezing problem has shown that high accuracy computations can be executed on grids with a small number of nodes.

1. Introduction

The principal complexity of mathematical studies of Stefan-like problems is due to the presence of moving boundaries which leads to substantial nonlinearity. An analytic solution of such problems can be obtained only under strong simplifying assumptions. Two approaches are widely used to solve the Stefan problems numerically: determination of a classical solution with explicit tracking of the moving surface of discontinuity [1 - 3] and determination of the generalized solution by means of the smoothing procedure using a smoothing calculation scheme [4 - 6]. The algorithms of smoothing have come into a widespread use and have proved to be especially effective in multidimensional statements. However, introduction of the smoothing procedure completely excludes from consideration the interface and physical phenomena involved, for example, the kinetics of phase transition. This imposes natural restrictions on the area of applicability of the given approach. In problems of pulse action of high-energy fluxes on materials where the nonequilibrium of fast phase transformations can play a dominant role, and also in a number of other applications, it is necessary to locate explicitly the phase-boundaries and to take into account the related processes. The leading position of smoothing calculation algorithms in multidimensional problems is greatly the due to the lack of effective methods of solution with explicit tracking of moving boundaries. In the present work the solution of the classical version of the two-dimensional nonstationary Stefan problem with explicit tracking of the interface is considered. The solution is carried out by means of the dynamic adaptation method [7 - 8] widely used for the solution of nonstationary one-dimensional problems of mathematical physics.

The dynamic adaptation method is based on the idea of transition to an arbitrary nonstationary coordinate system, which is controlled by the sought-for solution. In an arbitrary nonstationary coordinate system the problem is described by an extended set of differential equations one part of which describes the physical phenomenon and the other describes the dynamics of nodes of the calculated grid. In two-dimensional non-stationary problems the description of the movement of nodes is carried out by means of two partial equations.

2. Classic version of Stefan problem

The mathematical statement of the classical version of the Stefan problem is reduced to the nonlinear heat

[1] The work is supported by the Russian Fundamental Research Fund, grants 97-01-00942 and the Belarusian Fundamental Research Fund, grants F96-173.

transfer equation

$$\left[\frac{\partial H}{\partial t} = div[\lambda(T)gradT] + g = -\frac{\partial W_1}{\partial x} - \frac{\partial W_2}{\partial y} + g\right]_m, \; m = s, l, \tag{1}$$

$$H_m = c_p \rho_m T, \quad \left(W_1\right)_m = -\lambda_m(T)\frac{\partial T}{\partial x}, \quad \left(W_2\right)_m = -\lambda_m(T)\frac{\partial T}{\partial y}$$

in two subregions $\overline{\Omega}_s(t)$ and $\overline{\Omega}_l(t)$ divided by the a priori unknown boundary $\Gamma_{sl}(t)$. On the domain boundary $\overline{\Omega} = \overline{\Omega}_s \cup \overline{\Omega}_l$ the boundary conditions are specified in the form

$$(\vec{W}, \vec{n})|_{\partial\overline{\Omega}} = f,$$

where $\vec{W} = (W_1, W_2)$ is the vector of heat flow, $\vec{n}$ is the external normal to $\partial\overline{\Omega}$, f is specified on the $\partial\overline{\Omega}$ function. On the $\Gamma_{sl}(t)$ phase-boundary the differential Stefan condition is fulfilled:

$$W_l^n - W_s^n = L_m \rho v_{sl}^n, \quad W_s^\tau = W_l^\tau. \tag{2}$$

Except the Stefan condition on the $\Gamma_{sl}(t)$ boundary the constancy of transition temperature is also supposed:

$$T_s = T_l = T_m. \tag{3}$$

Here the indices n and τ indicate normal and tangent components, the s and l indices refer to solid and liquid phases, T_m, L_m are the temperature and latent heat of melting/crystallization, v_{sl} is the velocity of motion of the interface. The solution of the classical Stefan problem consists of determination of temperature fields and velocity of the phase front v_{sl}. The algorithm for numerical solution of realistic Stefan problems describing melting-solidification processes is split naturally into two qualitatively different stages. The first one relates to calculation of temperature fields in the absence of phase transformations and describes the heating up of the solid to the equilibrium melting temperature T_m and cooling down to the initial temperature T_0 after termination of the solidification process. The second stage relates to the determination of temperature fields in two subregions $\overline{\Omega}_s, \overline{\Omega}_l$ and the velocity of interface boundary.

3. Problem statement in an arbitrary curvilinear unsteady coordinate system

In solution of multidimensional boundary-value problems in the domains of arbitrary form the finite difference approximation of the differential equations is more convenient to perform in curvilinear coordinate systems. The type of a curvilinear coordinate system is determined by the requirements and restrictions imposed on the calculated grid by the solution of a specific problem. All restrictions can conditionally be divided into two categories. One of them is determined by the physical features of the processes considered, the other is concerned with the form and geometric parameters of the domain. Frequently both categories of restrictions take place simultaneously. The most rigid restrictions result from the approximation of boundary conditions in the case of problems with an arbitrary shape of the domain. The most suitable curvilinear coordinate systems for such situations are those in which the domain boundaries coincide the segments of coordinate lines. If the boundaries of a computational domain lie on the coordinate lines it eliminates additional interpolation procedure for approximation of boundary conditions of any type.

As already mentioned, the solution of the Stefan problem includes two stages. The basic feature of the first stage consists in the possible formation of large gradients near the heating zone of an external fixed source. The characteristic properties of the second stage are concerned with the emergence of moving phase-boundaries that are determined by the behavior of the velocity v_{sl}. These features should be taken into account in construction of computational grids. For the problem with an arbitrary shape of the domain, the specific features of the first stage can be accounted for by transition to curvilinear coordinates and concentration of coordinate lines in the heating zone. The situation is much more complicated for the second stage.

Apart from the difficulties concerned with the moving boundary, additional complications arise from variation of the characteristic sizes of the phases. At the onset of melting the originating phase includes only several atomic layers and its characteristic thickness is of an order of 10A. As time goes on, the thickness of the new phase increases by 3-6 orders of magnitude. The size of the initial phase changes similarly but in inverse direction. In this situation it appears that the computation grid used in the beginning of calculations becomes unsuitable after a certain period of time. To continue the calculation it is necessary to rebuild the grids radically. Taking into account the features explained, the construction of effective computational grids

in Stefan problems is possible only on the basis of adaptive approaches when an adaptive grid is dynamically coupled with the sought-for solution.

The indicated requirements are fully met by the dynamic adaptation method [3,9,10] in which application of the arbitrary nonstationary curvilinear coordinate system permits one to follow the motion of any element of physical space. The word "arbitrary" means that the law of the coordinate system motion is not specified beforehand as, for example, in the Lagrangian approach and is determined in the course of the solution. As a result, the movement of the nodes of the adaptive grid depends on evolution of the numerical solution of the physical problem. In particular, in the case of Stefan problems the dynamics of nodes becomes coupled with the velocity of phase front propagation. The inverse transformation for spatial variables in the method of dynamic adaptation is carried out by means of the two nonstationary partial differential equations. Thus, the required grid functions and the coordinates of grid nodes are determined simultaneously from the solution of unified partial differential model.

To map the physical space with the coordinates (x, y, t) into a computational one with (ξ, η, τ) we shall apply general transformation

$$\xi = \xi(x, y, t), \quad \eta = \eta(x, y, t), \quad \tau = t. \tag{4}$$

The classical Stefan problem in the arbitrary nonstationary curvilinear coordinate system (ξ, η, τ) can be written in the form:

$$\Big[\frac{\partial}{\partial\tau}(\psi H) = \frac{\partial}{\partial\xi}[(\rho W_1 + HQ_1)\frac{\partial y}{\partial\eta} - (\rho W_2 + HQ_2)\frac{\partial x}{\partial\eta}] - \tag{5}$$

$$-\frac{\partial}{\partial\eta}[-(\rho W_1 + HQ_1)\frac{\partial y}{\partial\xi} + (\rho W_2 + HQ_2)\frac{\partial x}{\partial\xi}] + \psi g\Big]_m, m = s, l,$$

$$\Big[\frac{\partial x}{\partial\tau} = -\frac{Q_1}{\rho}\Big]_m, \tag{6}$$

$$\Big[\frac{\partial y}{\partial\tau} = -\frac{Q_2}{\rho}\Big]_m \tag{7}$$

with the corresponding boundary conditions on the line of phase transition

$$Q^n_{sl} = -\rho v^n_{sl} = L^{-1}_m(W^n_s - W^n_l), \quad W^\tau_s = W^\tau_l, \tag{8}$$

$$T_s = T_l = T_m, \tag{9}$$

where (6), (7) are the equations of inverse transformation, $H_m = c_p\rho_m T$ is the enthalpy, W_1, W_2 are the heat fluxes

$$(W_1)_m = \Big(-\frac{\lambda\rho}{\psi}(\frac{\partial y}{\partial\eta}\frac{\partial T}{\partial\xi} - \frac{\partial y}{\partial\xi}\frac{\partial T}{\partial\eta})\Big)_m, \quad (W_2)_m = \Big(-\frac{\lambda\rho}{\psi}(-\frac{\partial x}{\partial\eta}\frac{\partial T}{\partial\xi} + \frac{\partial x}{\partial\xi}\frac{\partial T}{\partial\eta})\Big)_m,$$

Q_{sl} is the flow of substance through the interface, Q_1, Q_2 are the arbitrary transformation functions. The variables $\psi_m = \Big[\rho(\frac{\partial x}{\partial\xi}\frac{\partial y}{\partial\eta} - \frac{\partial x}{\partial\eta}\frac{\partial y}{\partial\xi})\Big]_m, \frac{\partial x}{\partial\xi}, \frac{\partial y}{\partial\xi}, \frac{\partial x}{\partial\eta}, \frac{\partial y}{\partial\eta}$ represent the Jacobian and metric transformation coefficients.

4. Transformation function $\vec{Q}$.

Similar to other problems of mathematical physics, the basic problems of construction of computational grids for the Stefan problem is to determine mapping transformation of a physical space into a computational one. As the solution of total Stefan problem includes two qualitatively different stages, two forms of mapping are used for construction of computational grids. Both transformations map the domain of arbitrary form $\overline{\Omega}$ of the physical space onto the rectangle Ω in the plane of curvilinear coordinates (ξ, η). Thus, in the computational space the mutually orthogonal coordinate lines will form a uniform grid with rectangular cells. In the physical space they correspond to the cells formed by intersection of nonuniformly located nonorthogonal coordinate lines. All the boundaries in the computational space including the moving ones conjugate with the segments of the coordinate lines. The solution of problem (1)—(3) in heating - cooling stages without phase transformations does not differ from the solution of typical nonstationary problems of mathematical physics.

To construct fixed (nonreconstructed) grids a rather simple and commonly used technique is applied, and necessary mapping is determined by means of the numerical solution of a system of special elliptic (Poisson type) equations [11]. Thus, the solution of the first stage of the problem will be carried out on a fixed grid

constructed before the beginning of calculations. The grid nodes are concentrated toward the heating zone by special choice of P_1 and P_2 functions on the right side of the Poisson equations.

The second stage of the solution deals with the formation and propagation of the $\Gamma_{sl}(t)$ phase boundary. Application of a nonstationary coordinate system in the computational space makes the $\Gamma_{sl}(t)$ line of phase transition fixed and locates on one of coordinate lines. On this boundary the flow of matter $Q^n_{sl} = -\rho v^n_{sl}$ is calculated by means of the boundary conditions (8) which define the mass flow from one subregion into another. In the physical space the grids in both subregions $\overline{\Omega}_s, \overline{\Omega}_l$ are rebuilt on each time layer in accordance with a magnitude and sign of the mass flow. The arbitrariness of the transformation functions Q_1, Q_2 means that all the points of the physical space move with their own velocities which makes it possible to adapt the computational grid to any features of the sought-for solution. In particular, it is reasonable for the Stefan problems to require that the nodes of the computational grids at every time instant be distributed quasi-uniformly in every direction. To reach this objective the Q_1, Q_2 functions can be selected in the form:

$$Q_1 = -\rho\left(D_\xi \frac{\partial^2 x}{\partial \xi^2} + D_\eta \frac{\partial^2 x}{\partial \eta^2}\right), \quad Q_2 = -\rho\left(D_\xi \frac{\partial^2 y}{\partial \xi^2} + D_\eta \frac{\partial^2 y}{\partial \eta^2}\right), \tag{10}$$

where the D_ξ, D_η quantities depend on the velocity of the phase front nodes and degree of subdomains transformation.

5. Generation of grids

The problem of grid generation consists in the determination of coupling between the (ξ, η) points of the regular computational domain Ω and the (x, y) points of the domain $\overline{\Omega}$ (Fig. 1).

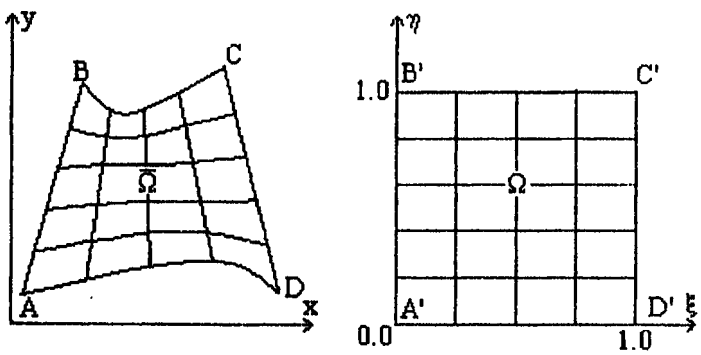

Fig. 1. Mapping of the initial space into the computational space.

Stage 1. For the construction of moving grids in arbitrary two-dimensional domains the method based on the solution of elliptical equations [11] is used:

$$\frac{\partial^2 \xi}{\partial x^2} + \frac{\partial^2 \xi}{\partial y^2} = P_1(\xi, \eta), \quad \frac{\partial^2 \eta}{\partial x^2} + \frac{\partial^2 \eta}{\partial y^2} = P_2(\xi, \eta), \quad (x, y) \in \overline{\Omega}. \tag{11}$$

Here $P_1(\xi, \eta)$, $P_2(\xi, \eta)$ are the functions used to control the concentration of the internal nodes of the grid. Equations (11) are solved in the Ω domain in which they have the following form

$$\alpha \frac{\partial^2 x}{\partial \xi^2} - 2\beta \frac{\partial^2 x}{\partial \xi \partial \eta} + \gamma \frac{\partial^2 x}{\partial \eta^2} + J^2\left(P_1 \frac{\partial x}{\partial \xi} + P_2 \frac{\partial x}{\partial \eta}\right) = 0, \tag{12}$$

$$\alpha \frac{\partial^2 y}{\partial \xi^2} - 2\beta \frac{\partial^2 y}{\partial \xi \partial \eta} + \gamma \frac{\partial^2 y}{\partial \eta^2} + J^2\left(P_1 \frac{\partial y}{\partial \xi} + P_2 \frac{\partial y}{\partial \eta}\right) = 0, \tag{13}$$

where

$$\alpha = \left(\frac{\partial x}{\partial \eta}\right)^2 + \left(\frac{\partial y}{\partial \eta}\right)^2, \quad \beta = \frac{\partial x}{\partial \xi}\frac{\partial x}{\partial \eta} + \frac{\partial y}{\partial \xi}\frac{\partial y}{\partial \eta}, \quad \gamma = \left(\frac{\partial x}{\partial \xi}\right)^2 + \left(\frac{\partial y}{\partial \xi}\right)^2,$$

$$J = \frac{\partial(x, y)}{\partial(\xi, \eta)} = \frac{\partial x}{\partial \xi}\frac{\partial y}{\partial \eta} - \frac{\partial x}{\partial \eta}\frac{\partial y}{\partial \xi}.$$

The set of equations (12)—(13) is supplemented with the boundary conditions characterizing the distribution of nodes on the $\partial\overline{\Omega}$ boundary of the physical domain:

$$(x,y)_{AB} = (x(\xi,\eta), y(\xi,\eta))|_{\eta\in A'B'}, \quad (x,y)_{BC} = (x(\xi,\eta), y(\xi,\eta))|_{\xi\in B'C'},$$

$$(x,y)_{CD} = (x(\xi,\eta),\ y(\xi,\eta))|_{\eta\in C'D'}, \quad (x,y)_{DA} = (x(\xi,\eta),\ y(\xi,\eta))|_{\xi\in D'A'}.$$

The distribution of the grid nodes on the AB, BC, CD and DA segments of the $\partial\overline{\Omega}$ boundary is determined by means of the two-parametric stretching function of Vinokur $s(t,p,q)$ [12]. Choice of p and q parameters representing the declination of the function $s(t,p,q)$ on the boundaries of the interval $0 \le t \le 1$ permits one to reach the required concentration of the grid nodes on the $\partial\overline{\Omega}$ boundary: $p = q = 1$ leads to equidistant distribution, $p, q < 1$ gives concentration inward the segment, $p, q > 1$ gives concentration toward the boundaries of the segment, $p > 1$, $q < 1$ and $p < 1$, $q > 1$ concentrate nodes toward the beginning and end of the segment. The P_1 and P_2 functions control the concentration of the grid nodes inside the $\overline{\Omega}$ area and are selected in the form [11]:

1) $P_1(\xi,\eta) = P_2(\xi,\eta) = 0$ for the quasi-equidistant distribution,

2) $P_1(\xi,\eta) = -asign(\xi-\xi_i)exp(-b|\xi-\xi_i|)$ for the concentration of the lines $\xi = const$ to the line $\xi = \xi_i$,

3) $P_2(\xi,\eta) = -asign(\eta-\eta_k)exp(-b|\eta-\eta_k|)$ for the concentration of the lines $\eta = const$ to the line $\eta = \eta_k$.

The concentration of the lines of the grid $\xi = const$ and $\eta = const$ to the point (ξ_i, η_k) is reached by defining the P_1 and P_2 functions in the form

$$P_1(\xi,\eta) = -asign(\xi-\xi_i)exp(-b[(\xi-\xi_i)^2 + (\eta-\eta_k)^2]^{1/2}),$$

$$P_2(\xi,\eta) = -asign(\eta-\eta_k)exp(-b[(\xi-\xi_i)^2 + (\eta-\eta_k)^2]^{1/2}).$$

The $a, b \ge 0$ coefficients are selected in such a way as to obtain the required grid parameters. The differential equation (12) on the equidistant grid in the Ω area is approximated by means of central differences that lead to following difference scheme

$$\alpha'(x_{i-1,k} - 2x_{i,k} + x_{i+1,k}) - 0.5\beta'(x_{i+1,k+1} - x_{i-1,k+1} - x_{i+1,k-1} + x_{i-1,k-1}) + \gamma'(x_{i,k-1} - 2x_{i,k} + x_{i,k+1}) +$$

$$+0.5\delta' P_1(x_{i+1,k} - x_{i-1,k})/h_\xi + 0.5\delta' P_2(x_{i,k+1} - x_{i,k-1})/h_\eta = 0,$$

where

$$\alpha' = 0.25[(x_{i,k+1} - x_{i,k-1})^2 + (y_{i,k+1} - y_{i,k-1})^2],$$

$$\beta' = 0.25[(x_{i+1,k} - x_{i-1,k})(x_{i,k+1} - x_{i,k-1}) + (y_{i+1,k} - y_{i-1,k})(y_{i,k+1} - y_{i,k-1})],$$

$$\gamma' = 0.25[(x_{i+1,k} - x_{i-1,k})^2 + (y_{i+1,k} - y_{i_1,k})^2],$$

$$\delta' = 0.0625[(x_{i+1,k} - x_{i-1,k})(y_{i,k+1} - y_{i,k-1}) - (x_{i,k+1} - x_{i,k-1})(y_{i+1,k} - y_{i-1,k})]^2.$$

Equation (13) is approximated similarly. To solve the equations obtained the Newton iterative procedure is used.

Stage 2. The construction of moving computational grids have been carried out by means of the numerical solution of the nonstationary equations (6), (7) which, accounting for Eq. (10), take the form:

$$\frac{\partial x}{\partial \tau} = D_\xi \frac{\partial^2 x}{\partial \xi^2} + D_\eta \frac{\partial^2 x}{\partial \eta^2}, \quad \frac{\partial y}{\partial \tau} = D_\xi \frac{\partial^2 y}{\partial \xi^2} + D_\eta \frac{\partial^2 y}{\partial \eta^2}.$$

6. Algorithm of solution

For the finite difference approximation of Eqs. (5) - (7) in the $\Omega \times [0, t_0]$ domain of the generalized coordinates ξ, η, τ we shall introduce the rectangular grid ω with the steps $h_\xi, h_\eta, \Delta\tau^j$, respectively:

$$\omega = \left\{(\xi_i, \eta_k, \tau^j),\ \xi_{i+1} = \xi_i + h_\xi, i = 0,\dots,I-1,\ \eta_{k+1} = \eta_k + h_\eta, k = 0,\dots,K-1,\ \tau^{j+1} = \tau^j + \Delta\tau^j\right\}.$$

The functions $x^j_{i,k}, y^j_{i,k}, Q^j_{1,i,k}, Q^j_{2,i,k}$ are determined at the grid nodes, while the functions $T^j_{i+1/2,k+1/2}$, $\psi^j_{i+1/2,k+1/2}$, $H^j_{1,i+1/2,k+1/2}$ are evaluated at the cell centers. The variables $W^j_{1,i+1/2,k}$, $W^j_{2,i+1/2,k}$, $W^j_{1,i,k+1/2}$,

$W^j_{2,i,k+1/2}$ are evaluated at the centers of the cell edges. Using the integro-interpolational method [13] the initial differential problem (2) is approximated by means of the implicit difference scheme:

$$\frac{(\psi H)^{j+1}_{i+1/2,k+1/2} - (\psi H)^j_{i+1/2,k+1/2}}{\Delta\tau^j} = -\frac{1}{h_\xi h_\eta}\Big\{(\rho W_1 + HQ_1)_{i+1,k+1/2}(y_{i+1,k+1} - y_{i+1,k}) -$$
$$-(\rho W_1 + HQ_1)_{i,k+1/2}(y_{i,k+1} - y_{i,k}) - (\rho W_1 + HQ_1)_{i+1/2,k+1}(y_{i+1,k+1} - y_{i,k+1}) +$$
$$+(\rho W_1 + HQ_1)_{i+1/2,k}(y_{i+1,k} - y_{i,k}) - (\rho W_2 + HQ_2)_{i+1,k+1/2}(x_{i+1,k+1} - x_{i+1,k}) -$$
$$-(\rho W_2 + HQ_2)_{i,k+1/2}(x_{i,k+1} - x_{i,k}) - (\rho W_2 + HQ_2)_{i+1/2,k+1}(x_{i+1,k+1} - x_{i,k+1}) +$$
$$+(\rho W_2 + HQ_2)_{i+1/2,k}(x_{i+1,k} - x_{i,k})\Big\}^{j+1} - (\psi g)^{j+1}_{i+1/2,k+1/2}.$$

Here

$$W_{1,i+1/2,k} = -\frac{\lambda\rho}{\psi_{i+1/2,k}h_\xi h_\eta}\left\{(y_{i+1/2,k+1/2} - y_{i+1/2,k-1/2})(T_{i+1,k} - T_{i,k}) -\right.$$
$$\left.-(y_{i+1,k} - y_{i,k})(T_{i+1/2,k+1/2} - T_{i+1/2,k-1/2})\right\},$$
$$W_{1,i,k+1/2} = -\frac{\lambda\rho}{\psi_{i,k+1/2}h_\xi h_\eta}\left\{(y_{i,k+1} - y_{i,k})(T_{i+1/2,k+1/2} - T_{i-1/2,k+1/2}) -\right.$$
$$\left.-(y_{i+1/2,k+1/2} - y_{i-1/2,k+1/2})(T_{i,k+1} - T_{i,k})\right\},$$
$$W_{2,i+1/2,k} = -\frac{\lambda\rho}{\psi_{i+1/2,k}h_\xi h_\eta}\left\{-(x_{i+1/2,k+1/2} - x_{i+1/2,k-1/2})(T_{i+1,k} - T_{i,k}) +\right.$$
$$\left.+(x_{i+1,k} - x_{i,k})(T_{i+1/2,k+1/2} - T_{i+1/2,k-1/2})\right\},$$
$$W_{2,i,k+1/2} = -\frac{\lambda\rho}{\psi_{i,k+1/2}h_\xi h_\eta}\left\{-(x_{i,k+1} - x_{i,k})(T_{i+1/2,k+1/2} - T_{i-1/2,k+1/2}) +\right.$$
$$\left.+(x_{i+1/2,k+1/2} - x_{i-1/2,k+1/2})(T_{i,k+1} - T_{i,k})\right\},$$
$$\psi_{i+1/2,k+1/2} = \frac{\rho}{2h_\xi h_\eta}\{(x_{i+1,k} - x_{i,k+1})(y_{i+1,k+1} - y_{i,k}) - (x_{i+1,k+1} - x_{i,k})(y_{i+1,k} - y_{i,k+1})\}.$$

The required interpolation is performed by means of the following formulas:

$$H_{i,k+1/2} = 0.5(H_{i+1/2,k+1/2} + H_{i-1/2,k+1/2}),$$
$$H_{i+1/2,k} = 0.5(H_{i+1/2,k+1/2} + H_{i+1/2,k-1/2}),$$
$$Q_{i,k+1/2} = 0.5(Q_{i,k+1} + Q_{i,k}),\ Q_{i+1/2,k} = 0.5(Q_{i+1,k} + Q_{i,k}),$$
$$x_{i+1/2,k+1/2} = 0.25(x_{i,k} + x_{i,k+1} + x_{i+1,k} + x_{i+1,k+1}),$$
$$y_{i+1/2,k+1/2} = 0.25(y_{i,k} + y_{i,k+1} + y_{i+1,k} + y_{i+1,k+1}).$$

To realize the difference scheme, algorithm based on two enclosed iteration cycles have been used on each time step $\Delta\tau^j$. In the first cycle the $Q_{i,k}$ velocities of the grid nodes and their position have been determined and in second the distribution of temperatures in the domains $\overline{\Omega}_l, \overline{\Omega}_s$ have been calculated. The systems of the linear algebraic equations obtained were solved by means of the method referred to in [14]. The value of the normal component of the mass flow on the line of phase front ($\eta = \eta_{sl}$) in the edge centers of the cells is determined from the Stefan condition:

$$Q^n_{i+1/2,k_{sl}} = L_m^{-1}\left[(W^n_{i+1/2,k_{sl}})_s - (W^n_{i+1/2,k_{sl}})_l\right], i = 0, \ldots, I-1.$$

Here $(\cdot)^n$ is the normal component of the corresponding vector with respect to the line of phase front. The values $Q^n_{i+1/2,k_{sl}}$ have been interpolated to the nodes on the line of phase front by the formula $Q^n_{i,k_{sl}} = 0.5(Q^n_{i-1/2,k_{sl}} + Q^n_{i+1/2,k_{sl}})$. To provide more equidistant distribution of nodes on the line of phase front the tangential component of the mass flow $Q^\tau_{i,k_{sl}}$ was also determined. Finally, we obtained the following expression for the determination of $\vec{Q}_{i,k_{sl}} = (Q_{1,i,k_{sl}}, Q_{2,i,k_{sl}})$

$$\vec{Q}_{i,k_{sl}} = Q^n_{i,k_{sl}} \cdot \vec{n} + Q^\tau_{i,k_{sl}} \cdot \vec{\tau},$$

where $\vec{n}$ is the unit vector of the normal and $\vec{\tau}$ is the unit vector in the tangential direction to the phase front line. To determine the velocity components for the points of the phase front on the external boundary of the area $Q_{1,0,k_{sl}}, Q_{2,0,k_{sl}}, Q_{1,I,k_{sl}}, Q_{2,I,k_{sl}}$ the mass conservation law was used.

7. Freezing model problem

Verification of the dynamic adaptation method was carried out on the problem referred to in [4]. The Stefan problem for the process of freezing is considered in the rectangular domain $\overline{\Omega}: (0 \le x \le 1, 0 \le y \le 0.5)$ with the planar interface $\Gamma_{sl}(t)$ between $\overline{\Omega}_s(t)$ and $\overline{\Omega}_l(t)$ sub-domains. The coordinate axes were selected in such a way that the temperature of the moving phase boundary $\Gamma_{sl}(t)$ remains parallel to itself without being parallel to any of the axes (Fig. 2).

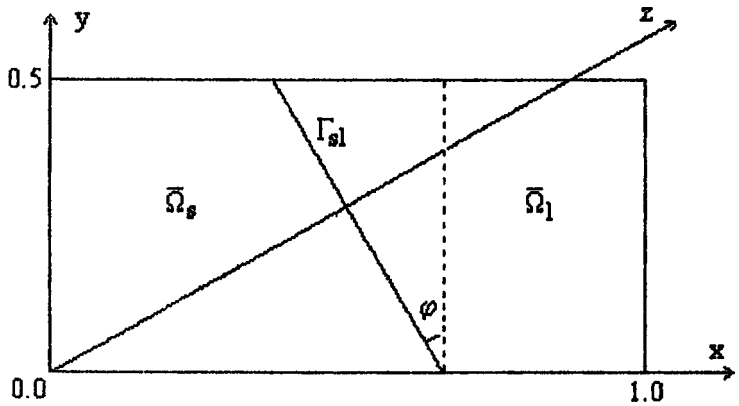

Fig. 2. Initial domain for the freezing problem.

The problem is described by the heat transfer equation (1) with constant coefficients. the following values of the thermophysical parameters were used: $\lambda = c = \rho = 1, L_m = 1, T_m = 0$. Turning the original coordinate system through the angle φ the problem is reduced to the one-dimensional Stefan problem with the spatial coordinate $z = x\cos\varphi + y\sin\varphi$, that has a self-similar solution:

$$T(z,t) = \begin{cases} -1 + \Phi\left(\frac{z}{2\sqrt{t}}\right)/\Phi(\beta), & 0 \le z \le z_\Gamma, \\ 0, & z > z_\Gamma, \end{cases}$$

where

$$\Phi(z) = \frac{2}{\sqrt{\pi}} \int_0^z e^{-y^2} dy, \quad z_\Gamma = 2\beta\sqrt{t}, \quad \beta = 0.6202.$$

The computational grid with an 11 x 6 total number of nodes was used. Initial distribution was selected to correspond to the self-similar solution at the time moment $t_0 = 0.162$. The planar boundary is drawn at the angle $\varphi = 30°$. Passing to the curvilinear coordinate system (ξ, η, τ) the $\overline{\Omega}$ domain is mapped into some rectangular domain Ω in which the computational grid becomes equidistant in both directions. The planar boundary $\Gamma_{sl}(\xi, \eta)$ coincides with the coordinate line $\eta_4, k_{sl} = 4$ and its position remains unchanged as time goes on (Fig. 3). The position of the phase front and the view of the computational grid in the physical space for different time moments are presented in Fig. 4.

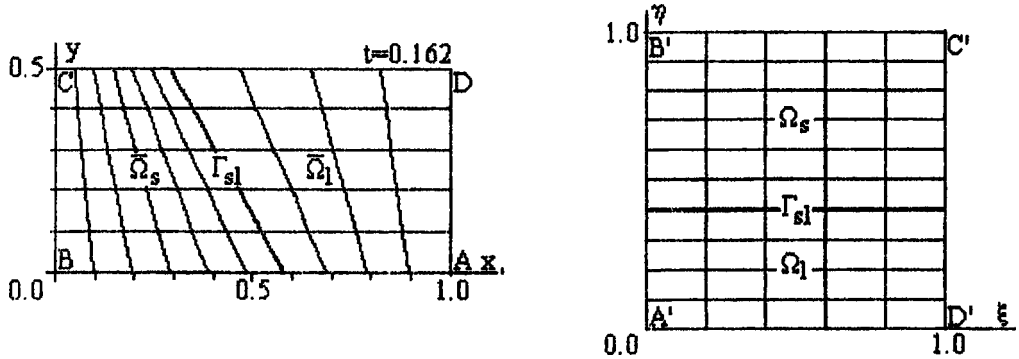

Fig. 3. Mapping of the physical space onto the computational one for freezing.

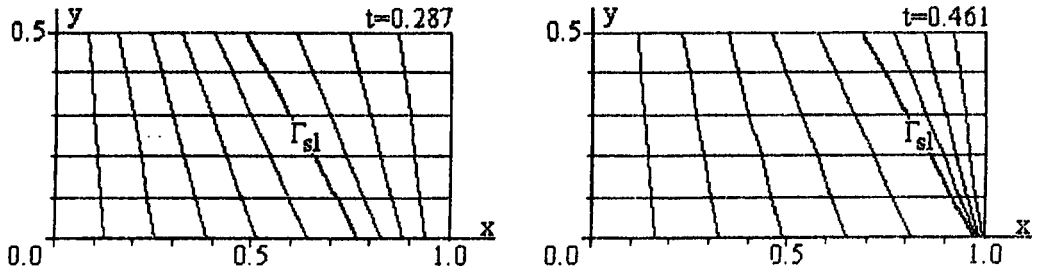

Fig. 4. Phase boundary position versus time for the freezing problem.

The values of the absolute error $\Delta z_i = z_i - z_\Gamma$ and relative error $\delta z_i = \Delta z_i / z_\Gamma$ in percentage are presented in Table 1 which describes a deviation of the phase-boundary from planar one for different time moments. Here z_Γ is the value of the coordinate z corresponding to the phase-boundary, z_i is the calculated value of the coordinate z corresponding to the position of the i-th node on the phase-boundary. The results obtained demonstrate a high accuracy of phase-boundary tracking and validate the application of the computational grid with a very small number of nodes, namely, about 10 in the Ω_s and Ω_l subdomains.

	$t = 0.2601, z(t) = 0.6326$			$t = 0.3363, z(t) = 0.7193$			$t = 0.4533, z(t) = 0.8351$		
i	z_i	Δz_i	δz_i	z_i	Δz_i	δz_i	z_i	Δz_i	δz_i
0	0.6337	$1.101 \cdot 10^{-3}$	0.1740	0.7203	$9.731 \cdot 10^{-4}$	0.1353	0.8362	$1.094 \cdot 10^{-3}$	0.1310
1	0.6340	$1.382 \cdot 10^{-3}$	0.2184	0.7210	$1.657 \cdot 10^{-3}$	0.2303	0.8363	$1.151 \cdot 10^{-3}$	0.1378
2	0.6337	$1.058 \cdot 10^{-3}$	0.1673	0.7212	$1.851 \cdot 10^{-3}$	0.2573	0.8385	$3.441 \cdot 10^{-3}$	0.4121
3	0.6330	$3.795 \cdot 10^{-4}$	0.0600	0.7197	$3.514 \cdot 10^{-4}$	0.0488	0.8350	$-5.612 \cdot 10^{-5}$	-0.0067
4	0.6339	$1.291 \cdot 10^{-3}$	0.2042	0.7211	$1.767 \cdot 10^{-3}$	0.2456	0.8374	$2.330 \cdot 10^{-3}$	0.2790
5	0.6342	$1.570 \cdot 10^{-3}$	0.2482	0.7211	$1.723 \cdot 10^{-3}$	0.2396	0.8370	$1.937 \cdot 10^{-3}$	0.2320

Table 1. Deviation between calculated and planar phase-boundaries obtained on an 11 × 6 computational grid.

8. Numerical experiment

Let us consider application of the suggested dynamic adaptation algorithm to solve the problem of action of a high-energy flux on a metal target. A rectangular energy pulse of diameter $3.8 \cdot 10^{-3} m$ and intensity $10^7 W/m^2$ is incident on the AD surface of the triangular domain $\overline{\Omega}$ perpendicularly to the surface. A computational grid with 19 × 18 nodes was constructed in the domain with the maximum concentration of nodes in the energy release zone (Fig. 5a). Thermophysical parameters close to those of lead were selected. The solution algorithm consists of two stages. At the first stage the entire domain is equal to the solid subdomain $\overline{\Omega} = \overline{\Omega}_s$ and the process is described by the heat transfer equation. A fixed computational grid (Fig. 5a) was constructed before the beginning of calculations and was used for temperature field calculation until the $T_{max} < T_m$ condition is fulfilled on the irradiated surface. Characteristic feature of the grid on this stage is a substantial concentration of the coordinate lines in the energy release zone.

At the second stage which begins when the equilibrium melting temperature T_m is reached on the surface, the processes are described by the two-phase Stefan model. To introduce the new (liquid) phase the overheating of the irradiated surface by 0.1 K is supposed. From the relation of the overheating energy and latent heat L_m the initial thickness of the liquid phase is determined (about 10^{-7} m) and the new subregion $\overline{\Omega}_l, \overline{\Omega} = \overline{\Omega}_s \cup \overline{\Omega}_l$ is introduced. From this time the grid is reconstructed on each time layer. The total number of nodes is equal to 19 × 23 with 19 × 6 nodes located in the new phase.

The melting process induces substantial reorganization of the grid in the solid phase which becomes quasi-equidistant in each direction (Fig. 5b). The view of the computational grid for later time moments is shown in Figs. 5c, 5d, when the characteristic sizes of the liquid phase becomes comparable with the size of the solid phase. In this period the quasi-uniformity condition can be fulfilled for the grid in the liquid phase only. The velocity v_{sl} versus time plot at the $i = 9, k = 5$ point is presented in Fig. 6. Fragments of the physical space immediately on introduction of the new phase are shown in Fig. 7 in an expanded scale. Temperature distribution in the liquid and solid phases is shown in Fig. 8.

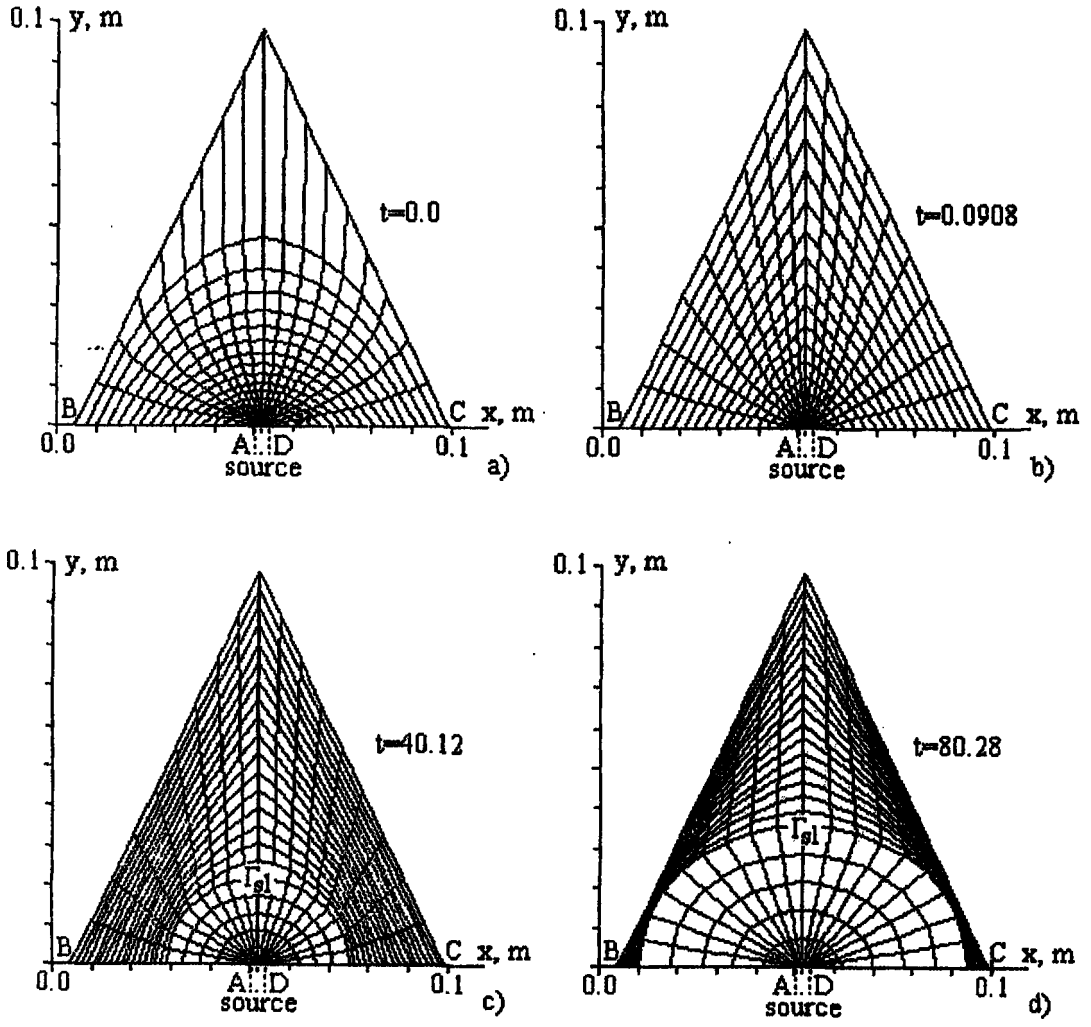

Fig. 5. The computational grid in the physical space.

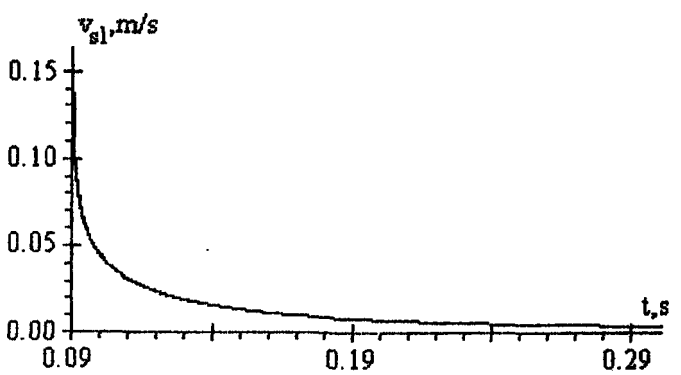

Fig. 6. Interface velocity versus time plot.

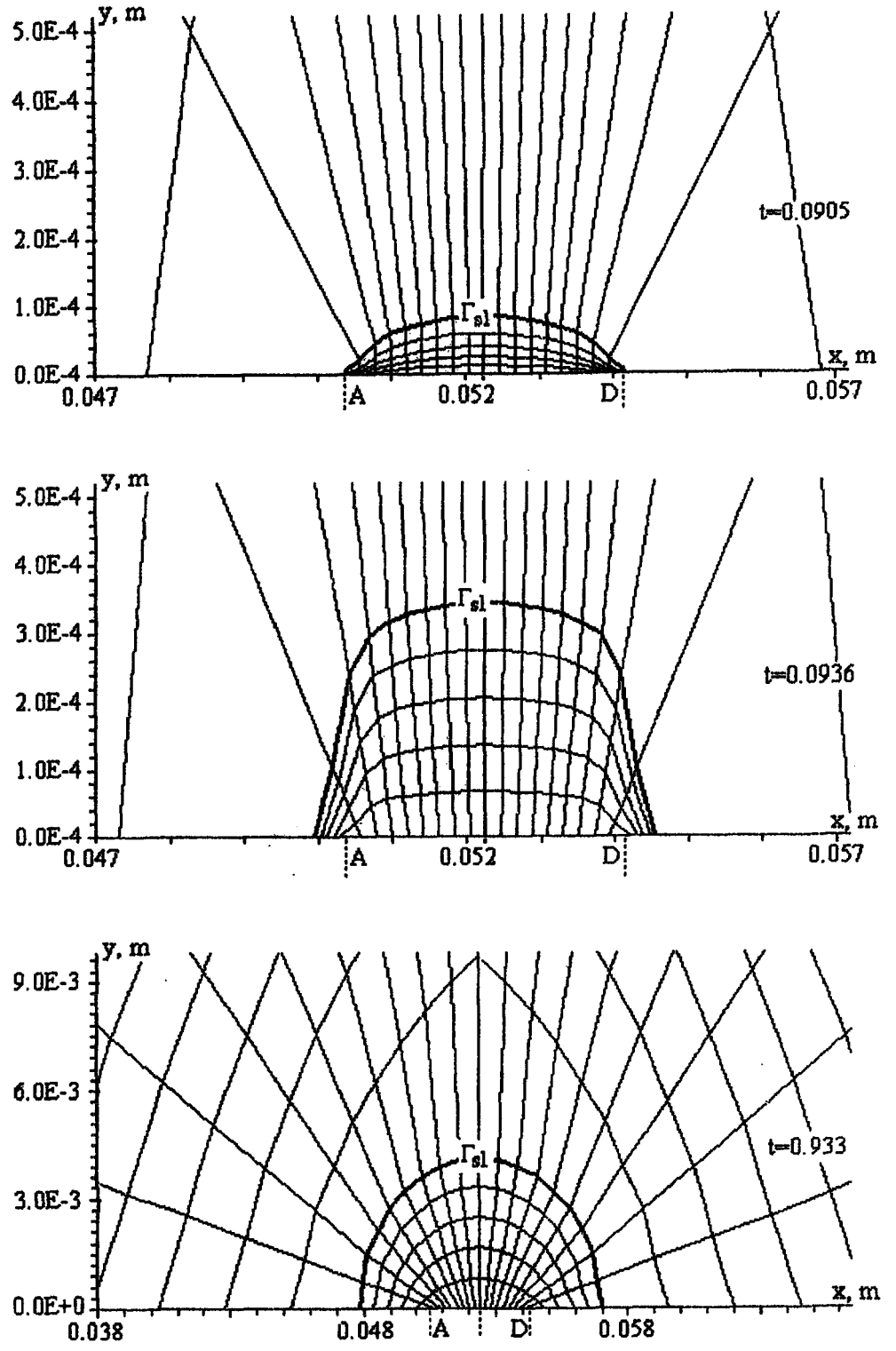

Fig. 7. Physical space fragment with the introduced liquid phase.

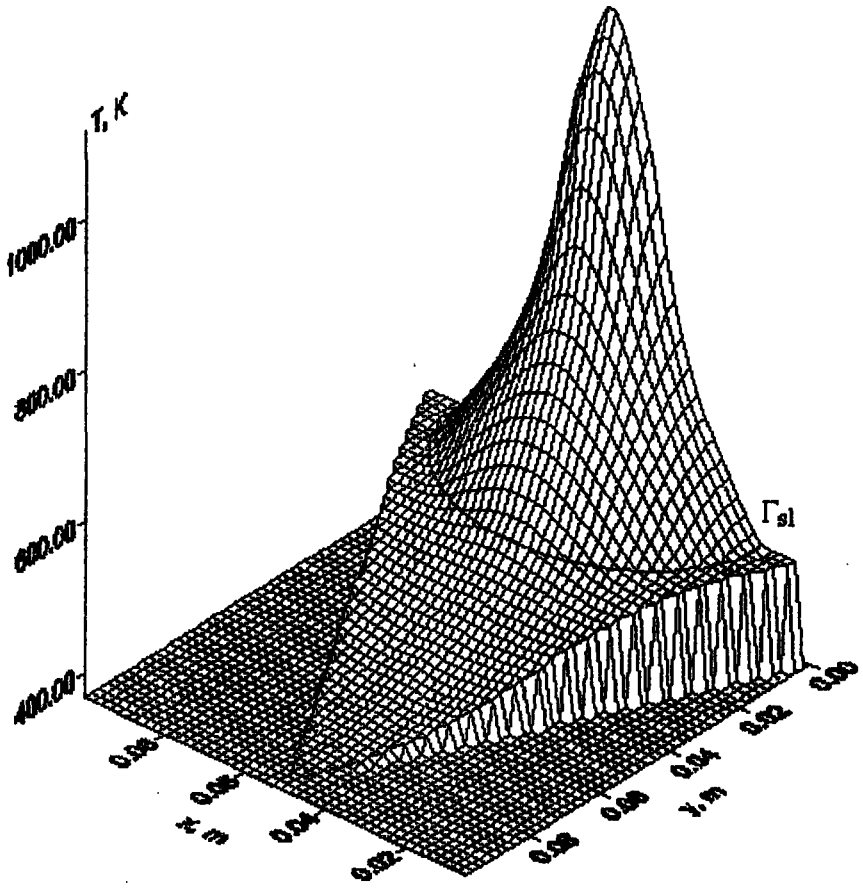

Fig. 8. Example of temperature distribution in the $\overline{\Omega}$ domain.

References

[1] M.Davis, P.Kapadia,J.Dowden, *Solution of a Stefan problem in the theory of laser welding by the method of lines*, Zh.Comput.Phys., **60** (1985), pp.534-548.

[2] F.P.Vasiliev, *About finite difference method for the solution of homogeneous Stefan problem*, Zh. Vychisl. Matem. i Matem. Fiz., **3** (1963), pp.861—873.

[3] P.V.Breslavskii, V.I.Mazhukin, *Mathematical modeling for pulse laser melting and evaporation processes of metals with explicit front-tracking*, Physical-Engineering J., **57** (1989), No. 1, pp. 107–114.

[4] A.A.Samarskii, G.D.Moiseenko, *Effective homogeneous scheme for multidimensional Stefan problem*, Zh. Vychisl. Matem. i Matem. Fiz., **5** (1965), No. 5. pp. 816–827.

[5] G.H.Meyer, *The numerical solution of Stefan problems with front-tracking and smoothing methods*, Appl. Math. Comput., **4** (1978), pp.283–306.

[6] B.R.E.White, *A modified finite difference scheme for the Stefan problem*, Math. Comput. **41** (1983), pp.816–827.

[7] N.A.Dar'in, V.I.Mazhukin, *One approach to adaptive grid generation*, Dokl. Akad. Nauk SSSR. **298** (1988), pp. 64–68.

[8] V.I.Mazhukin, A.A.Samarskii, Orlando Kastelianos, A.V.Shapranov, *The dynamic adaptation method for unsteady problems of mathematical physics with large gradients*, J. Math. Modeling, **5** (1993s), No. 4, pp. 33–56.

[9] N.A.Dar'in, V.I.Mazhukin, *Mathematical modeling of Stefan problem on adaptive grids*, J. Diff. Equations, **23** (1987), No. 7, pp. 1154–1160.

[10] N.A.Dar'in, V.I.Mazhukin, *Mathematical modeling of nonstationary two-dimensional boundary problem on dynamically adaptive grids*, Math. Modeling. **1** (1989), No 3, pp. 29–43.

[11] J.F.Thompson, Z.U.A.Warsi, C.W.Mastin, *Boundary fitted coordinate systems for numerical solution of partial differential equations - A review*, J.Comput.Phys., **47** (1982), pp.1–108.

[12] M.Vinokur, *On one-dimensional stretching functions for finite-difference calculations*, J.Comput.Phys., **50** (1983), pp.215– 234.

[13] A.A.Samarskii, **Theory of difference schemes.** (Nauka, 1977) (in Russian).

[14] G.E.Shneider, M.Zedan, *A modified strongly implicit procedure for the numerical solution of field problems*, Numer. Heat Transferm, **4** (1981), pp. 1–19.